

Research Article

X-Cut LiNbO₃ Optical Modulators Using Gap-Embedded Patch-Antennas for Wireless-Over-Fiber Systems

Yusuf Nur Wijayanto,¹ Hiroshi Murata,¹ Tetsuya Kawanishi,² and Yasuyuki Okamura¹

¹Division of Advanced Electronics and Optical Science, Department of Systems Innovation, Graduate School of Engineering Science, Osaka University, 1-3 Machikaneyama, Toyonaka, Osaka 560-8531, Japan

²Lightwave Device Laboratory, Photonic Network Research Institute, National Institute of Information and Communications Technology, 4-2-1 Nukui-Kitamachi, Koganei, Tokyo 184-8795, Japan

Correspondence should be addressed to Yusuf Nur Wijayanto, wijayanto@ec.ee.es.osaka-u.ac.jp

Received 15 July 2012; Accepted 17 September 2012

Academic Editor: Borja Vidal

Copyright © 2012 Yusuf Nur Wijayanto et al. This is an open access article distributed under the Creative Commons Attribution License, which permits unrestricted use, distribution, and reproduction in any medium, provided the original work is properly cited.

We propose an *x*-cut LiNbO₃ optical modulator using gap-embedded patch-antennas for wireless-over-fiber systems. The proposed device is composed of an array of narrow-gap-embedded patch-antennas and an optical waveguide located at the center of the gap without a buffer layer. The modulation efficiency of the proposed *x*-cut LiNbO₃ optical modulators was enhanced by 6 dB compared to the *z*-cut LiTaO₃-based devices.

1. Introduction

Wireless-over-fiber technology suitably supports wireless communication systems in microwave/millimeter-wave bands by compensating for large transmission losses of metallic cables [1]. In wireless-over-fiber technology for communication systems, microwave/millimeter-wave signals are converted to lightwave signals and transferred through optical fibers with low transmission loss. Large transmission bandwidth and no induction are also advantages of the optical fibers [2]. The wireless-over-fiber systems are composed of two domains: one is a microwave/millimeter-wave domain and the other is an optical domain. Therefore, conversion devices between the microwave/millimeter-wave and optical signals are required to realize the wireless-over-fiber systems.

A microwave/millimeter-wave generation for downlink in wireless-over-fiber systems can be achieved by a high-speed photodiode [3]. On the contrary for uplink conversion, the microwave/millimeter-wave signals can be directly converted into lightwave signals by use of high-speed optical modulation technology [4].

A conversion device from wireless microwave to lightwave signals can be composed of wireless microwave antennas and electrooptic (EO) modulators [5]. Wireless microwave signals can be received by the antennas. The received signals are transferred to the EO modulators by a connection line such as coaxial cables. However, microwave signal distortion and decay might occur in the coaxial cables due to high-frequency operation.

In order to reduce the microwave signal distortion and realize a simple compact device, wireless microwave-lightwave signal converters using integration of wireless microwave antennas and optical modulators have been developed. Several EO modulators using antenna-coupled resonant modulation electrodes were reported [6–10]. They were composed of planar antennas for wireless microwave signal receiving, resonant electrodes for optical modulation, and their connection lines on an EO crystal as a substrate. The antennas, resonant electrodes, and connection lines should be tuned precisely to obtain good resonance and impedance matching conditions for effective conversion. However, the complete matching and precise tuning are difficult and the microwave distortion might be still induced through the coupling of them.

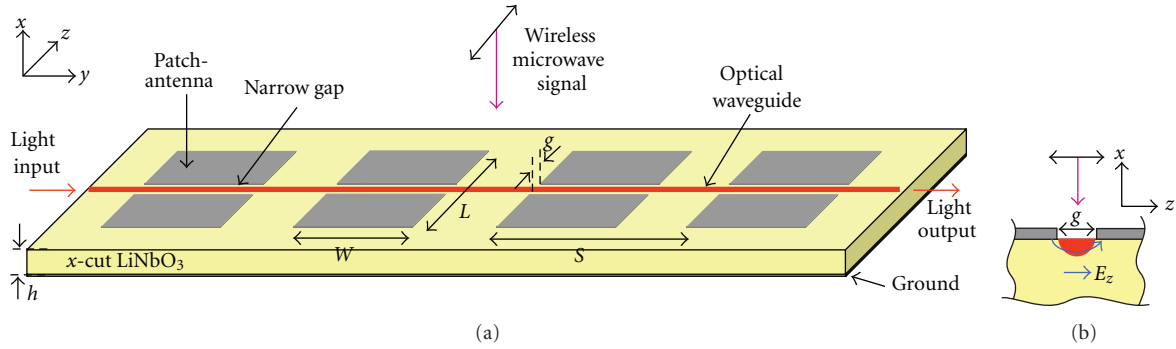


FIGURE 1: Schematic device structures of x -cut LiNbO_3 optical modulators using gap-embedded patch-antennas. (a) Whole device structure (3D view). (b) Cross-sectional view configuration of the device structure in xz -plane.

We have demonstrated EO modulators using patch-antennas embedded with narrow gaps on a z -cut LiTaO_3 crystal as the substrate [11–13]. The EO modulators are composed of patch-antennas only and there is no other planar structure on the substrate. They have no required precise tuning. Therefore, the optical modulation with extremely low distortion can be obtained with simple compact structures. Their basic operations were verified successfully with no external electrical power supply. However, modulation efficiency remains low due to large dielectric constant of the LiTaO_3 substrate and buffer layer structures in the devices.

In this paper, we propose a new x -cut LiNbO_3 optical modulator using gap-embedded patch-antennas for wireless microwave-lightwave signal conversion in the wireless-over-fiber systems. The proposed device is fabricated on z -cut LiNbO_3 with lower dielectric constant and no buffer layer structures. The basic operations of the proposed device were demonstrated experimentally at wireless microwave frequency of 26 GHz. Their modulation efficiency was enhanced by ~ 6 dB compared with the LiTaO_3 -based devices [12].

In the following sections, the device structure, operational principle, analysis, and experiments are presented.

2. Device Structures

Figure 1 shows the structure of the proposed x -cut LiNbO_3 optical modulator using gap-embedded patch-antennas. It consists of a channel optical waveguide and patch-antennas embedded with a narrow-gap onto an x -cut LiNbO_3 as the substrate. An array of the gap-embedded patch-antennas is set onto the substrate with a separation, S , which is key parameter to determine the characteristics in microwave-lightwave interactions described in the next section. The length, L , of each antenna along the x -axis is set as half a wavelength of the wireless microwave signal. The width, W , of each antenna along the y -axis is set as below one wavelength of the wireless microwave signal to avoid unwanted higher-order mode effects. The narrow gap in micrometer order is set at the centre of each antenna, along the y -axis. The optical waveguide is located at the center of the gap, where the magnified cross-sectional view is shown in

Figure 1(b). The reverse side of the substrate is covered with a ground electrode.

When a wireless signal is irradiated to a standard patch-antenna with no gap, a standing wave current is induced on the patch-antenna surface and becomes maximum at the center [14, 15]. With introducing a narrow gap at the center of the patch-antenna perpendicular to the surface current, a displacement current must be induced across the gap due to continuity of the current flow [16]. The strong electric field is also induced across the gap. When a lightwave propagates into an optical waveguide located under the gap, a lightwave is modulated by the wireless microwave signal through Pockels effects and the converted signal is obtained [17].

The optical modulation can be enhanced using the proposed device fabricated on the x -cut LiNbO_3 substrate. A buffer layer is not required. The dielectric constant of the x -cut LiNbO_3 along z -axis is about 28 and the LiTaO_3 is about 42. Therefore, strong electric field across the gap can be obtained using the proposed x -cut LiNbO_3 optical modulator. The efficiency enhancement is obtained by the lower dielectric constant of the substrate and no buffer layer.

3. Operational Principle

When a wireless microwave signal at the angular frequency ω_m is irradiated to the proposed device, the displacement current and strong electric field are induced across the narrow gap. The induced electric field is obtained by the time integration of the displacement currents [16]. The induced electric field can be expressed as

$$E_m^0(t) = E_{m0} \sin(\omega_m t). \quad (1)$$

When a lightwave propagates in the optical waveguide, the microwave electric field as would be observed by the lightwave can be expressed by the following equation taking into account the transit time of the lightwave [18, 19]:

$$\begin{aligned} E_{m\text{-opt}}^0(y) &= E_m^0 \left(\frac{y - y'}{v_g} \right) \\ &= E_{m0} \sin \left[k_m n_g y + \varphi \right], \end{aligned} \quad (2)$$

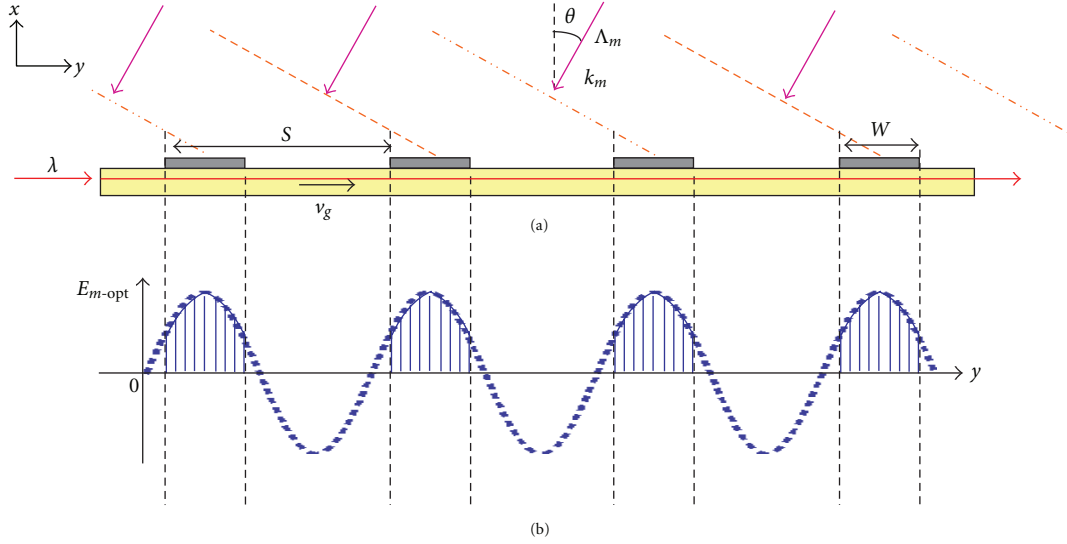


FIGURE 2: Operational principle of EO modulators. (a) Cross-sectional view under irradiation of a wireless microwave signal angle of θ degrees. (b) Microwave electric field observed by propagating lightwave along each gap-embedded patch-antenna. Modulation index corresponds to the shaded areas.

where k_m is the wave number of the microwave signal in vacuum ($k_m = \omega_m/c$), n_g is the group index of the lightwave propagating in the optical waveguide ($n_g = c/v_g$), v_g is the group velocity of the lightwave, c is the light velocity in vacuum, n_0 is the refractive index of the microwave in air ($=1$), and φ is an initial phase of the lightwave in the optical waveguide ($\varphi = k_m n_g y'$), corresponding to the phase of the microwave signal when the lightwave propagates in the optical waveguide.

For an array of gap-embedded patch-antennas as shown in Figure 2(a), the temporal phases of the microwave signal supplied to the gap-embedded patch-antennas are changed according to their separation, S , and the wireless irradiation angle, θ . The microwave electric field observed by the lightwave at h th gap-embedded patch-antennas, $E_{m\text{-opt}}^h$, can be expressed by

$$E_{m\text{-opt}}^h(y, \theta) = E_{m0} \sin[k_m n_g y + (h-1)S k_m n_0 \sin \theta + \varphi], \quad (3)$$

where

$$S = n v_g \frac{1}{\omega_m / 2\pi}, \quad (n: \text{integer}), \quad (4)$$

h denotes the number of the gap-embedded patch-antennas and S is a separation of the patch-antennas as shown in Figure 2.

The proposed device is an optical phase modulator. The modulation index is calculated from the integration of microwave electric field as would be observed by the

lightwave along the gap-embedded patch-antennas, it can be shown as

$$\Delta\phi(\theta) = \frac{\pi r_{33} n_e^3}{\lambda} \Gamma \sum_{h=1}^N \int_{(h-1)S}^{(h-1)S+W} E_{m\text{-opt}}^h(y, \theta) dy, \quad (5)$$

where λ is the wavelength of lightwave propagating in the optical waveguides, r_{33} is the EO coefficient, n_e is the extraordinary refractive index of the substrate, W are the width of the patch-antenna as the interaction length of the microwave and lightwave, N is the number of gap-embedded patch-antennas in the array structure, and Γ is a factor expressing the overlapping between the induced microwave electric field and the lightwave. The overlapping factor of the microwave and optical fields in the x - or z -components depends on the crystal orientation and optical field polarization. The modulation index of the proposed device corresponds to the sum of the shaded areas in Figure 2(b). Since the modulation index is also a function of wireless irradiation angle, θ , the directivity in the efficiency can be also calculated by (5).

4. Analysis

The details of the induced electric field across the gap in the proposed device using x -cut LiNbO₃ were analyzed. The device was designed for an operational frequency of 26 GHz. The thickness of the LiNbO₃ substrate was set as 0.5 mm. The size of the patch-antenna embedded with a 5 μm -wide gap was set to 0.7×1.3 mm for 26 GHz operation. The optical waveguide was designed 5 μm .

For comparison, an optical modulator with a gap-embedded patch-antenna using z -cut LiTaO₃ substrate was also analyzed. The thickness of the LiTaO₃ substrate was set

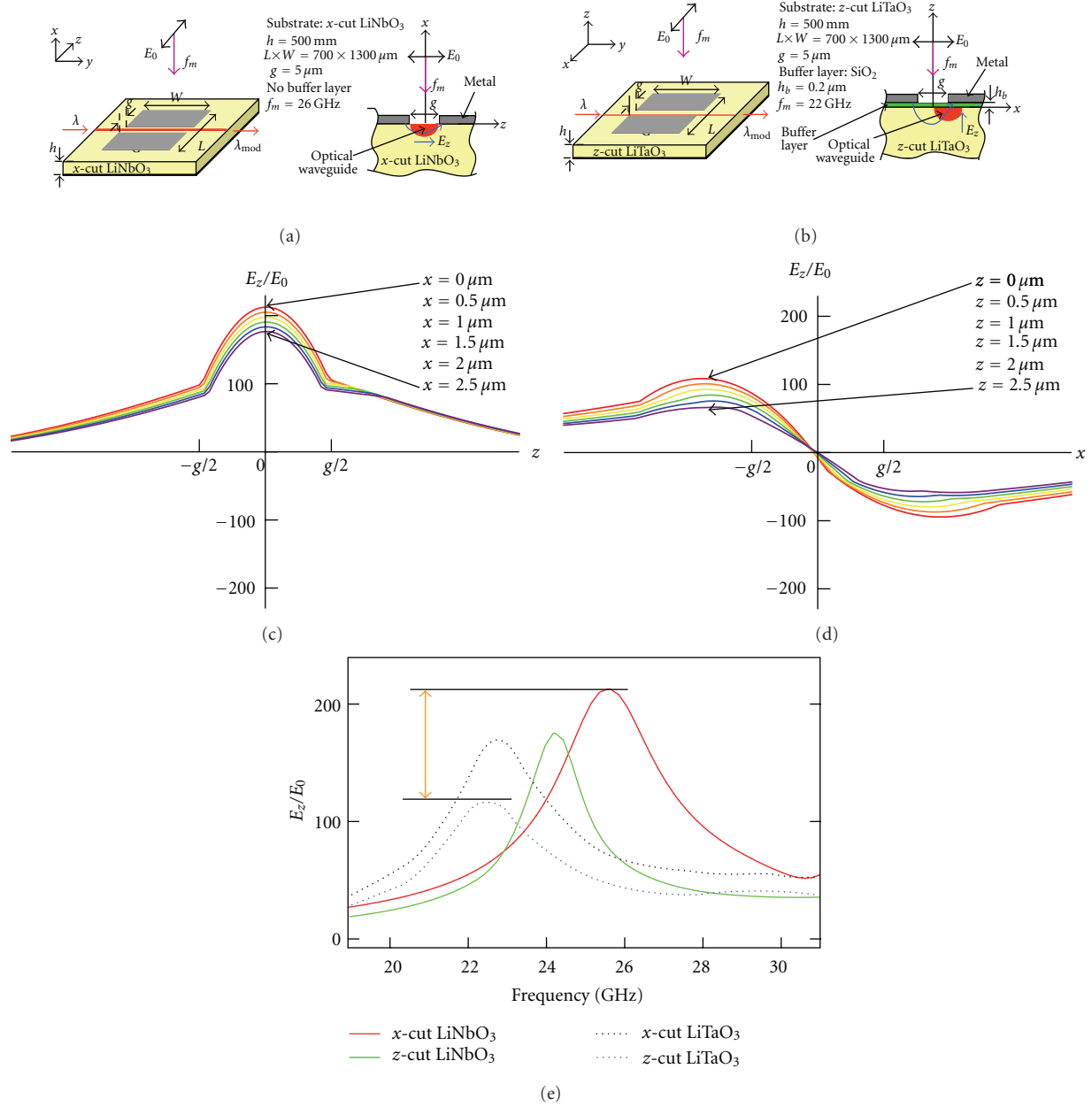


FIGURE 3: Microwave analysis of the optical modulators onto x -cut and z -cut of LiNbO_3 and LiTaO_3 substrates. (a) Structure of the device using x -cut LiNbO_3 . (b) Structure of the device using z -cut LiTaO_3 . (c) Calculated microwave electric field profile in the z -component for the device using x -cut LiNbO_3 . (d) Calculated microwave electric profile in the x -component for the device using z -cut LiTaO_3 . (e) Calculated frequency dependence of the maximum microwave electric for optical modulation.

as 0.5 mm. The size of the patch-antenna and gap were also set as $0.7 \times 1.3 \text{ mm}$ and $5 \text{ }\mu\text{m}$, respectively. However, the corresponding operational frequency becomes slightly small as 22 GHz owing to the large dielectric constant of LiTaO_3 along the z -axis.

Figures 3(a) and 3(b) show the cross-sectional views of the device configuration using x -cut LiNbO_3 and z -cut LiTaO_3 substrates. For the device using x -cut LiNbO_3 substrate, there is no buffer layer and the optical waveguide is located at the centre of the gap on the surface of the substrate

as shown in Figure 3(a). For the device using z -cut LiTaO_3 substrate, there is a $0.2 \text{ }\mu\text{m}$ -thick SiO_2 buffer layer and the optical waveguide is located under one side of the gap edge on the surface of the substrate as shown in Figure 3(b). The main microwave electric field components for driving EO effect are shown by the arrows in Figures 3(a) and 3(b), which are determined by the crystal orientation.

The microwave characteristics of the device were numerically analyzed using electromagnetic analysis software, HFSS. When a linearly polarized wireless microwave signal of E_0

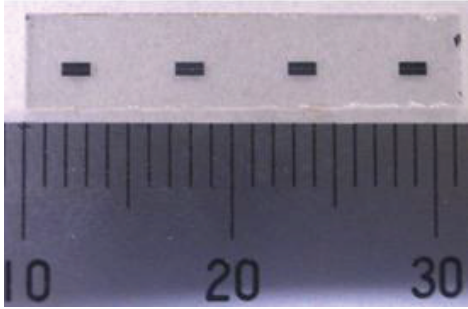


FIGURE 4: A photograph of a fabricated x -cut LiNbO_3 optical modulator using gap-embedded patch antennas before ground electrode fabrication.

perpendicular to the gap was irradiated to the devices, the microwave electric field profiles in the cross-section are shown in Figures 3(c) and 3(d). We can see that the strong microwave electric fields for optical modulation are obtained for device using: x -cut LiNbO_3 compared to z -cut LiTaO_3 -based device. We believe that these are due to the smaller dielectric constant and no buffer layer structure.

Figure 3(e) shows the calculated frequency dependence of the microwave electric field magnitude for optical modulation with the same patch-antennas size fabricated on different substrates, x -cut LiNbO_3 , z -cut LiNbO_3 , x -cut LiTaO_3 , and z -cut LiTaO_3 . They are indicated with colors of red, green, black, and blue, respectively. We can see that the largest electric field is induced for the x -cut LiNbO_3 device due to the smaller dielectric constant and no buffer layer structure. The peak resonant frequencies were slightly shifted owing to difference of dielectric constants in the LiNbO_3 and LiTaO_3 substrates.

The strong microwave electric field in the device using x -cut LiNbO_3 substrate can be used for optical modulation in the optical waveguide at the centre of the gap on the surface of the substrate. The modulation index can be calculated using (5). Considering the calculated microwave electric fields as shown in Figure 3(e), enhanced modulation index about two times can be obtained by using the x -cut LiNbO_3 device compared with the z -cut LiTaO_3 device, when the overlapping factor between the electric fields of the microwave and lightwave is almost same in both devices.

5. Experiments

The designed device was fabricated. First, a single-mode straight optical channel waveguide for the wavelength of $1.55 \mu\text{m}$ was fabricated by using titanium-diffused methods. A 4-element array of the gap-embedded patch-antennas were fabricated using a $1 \mu\text{m}$ -thick aluminum film on the substrate by use of thermal vapor deposition, a standard photolithography, and a lift-off technique. Finally, the reverse side of the device was covered using a $1 \mu\text{m}$ -thick aluminum film as a ground electrode. The photographs of the fabricated prototype device are shown in Figure 4.

The experimental setup for measuring basic operations of the fabricated device is shown in Figure 5. A $1.55 \mu\text{m}$

wavelength lightwave from a Distributed-Feed-Back (DFB) laser was passed through a lightwave polarizer and coupled to the fabricated device by use of an objective lens. A 26 GHz microwave signal from a microwave signal generator was irradiated to the fabricated device using a horn antenna with irradiated power of about 0.2 W. The output light spectrum was measured and monitored using an optical spectrum analyzer.

The examples of the output light spectra measured by an optical spectrum analyzer are shown in Figure 6, where the wireless microwave signal with frequency of 26 GHz was irradiated to the device normally ($\theta = 0$ degree). Figures 6(a) and 6(b) show measured output light spectra for the transverse electric (TE) and transverse magnetic (TM) modes of the lightwave, respectively, when a linearly-polarized wireless microwave signal with Z -polarization was irradiated. We can see that the optical modulation is more effective for TE-mode of the lightwave due to the larger EO effects in the z -direction of the LiNbO_3 . Figure 6(c) shows the output light spectrum when the polarization of the wireless microwave signal polarization was rotated with 90 degrees, which corresponds to Y -polarization. No optical sideband was observed for the Y -polarized wireless signal.

The measured frequency dependence of the modulation efficiency is shown by the dotted curve in Figure 7, when the irradiation angle of the wireless microwave signal was set normal to the device (0 degree) and the lightwave was set to TE-mode. The fabricated device was an optical phase modulator; therefore, a modulation index can be adopted as a measure for modulation efficiency. The modulation index can be calculated from the spectrum intensity ratio between the first sideband and the optical carrier as long as the modulation index value is rather smaller than unity. The peak frequency of the wireless microwave-optical conversion was about 25.7 GHz, which almost coincided with the calculated frequency dependence as shown by the red curve in Figure 7.

Figure 8 shows the measured dependence of modulation efficiency by the separation between the horn antenna and the fabricated device, S_d . The optical sidebands were observed with a range up to 1 m between the horn antenna and the device. In addition, the calculated far-field separation of ~ 80 mm for the fabricated device was obtained.

Figure 9 shows the measured irradiation angle dependence (directivity) of the fabricated device in the xy -plane. The measured directivity has good agreement with the theoretical calculation of the designed device.

The basic operations of the proposed device were demonstrated successfully. The enhanced modulation efficiency by 6 dB was obtained using the proposed x -cut LiNbO_3 optical modulators compared to the z -cut LiTaO_3 -based device as shown in Figure 10. The modulation efficiency of the proposed device can be enhanced further using photonic technology by the use of a sharp-cut optical filter and an optical amplifier [9].

In addition, the insertion loss of the device was measured approximately 11 dB by use of objective lenses as the lightwave coupling. They can be reduced by using optical fibers as the lightwave coupling. The insertion loss is not directly

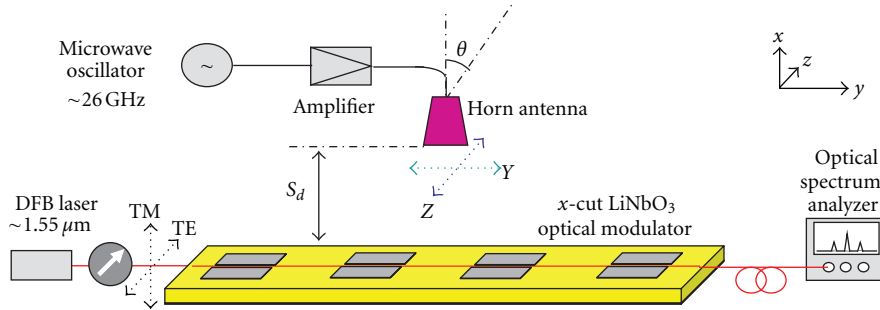


FIGURE 5: Experimental setup for measuring the operations of the fabricated optical modulators.

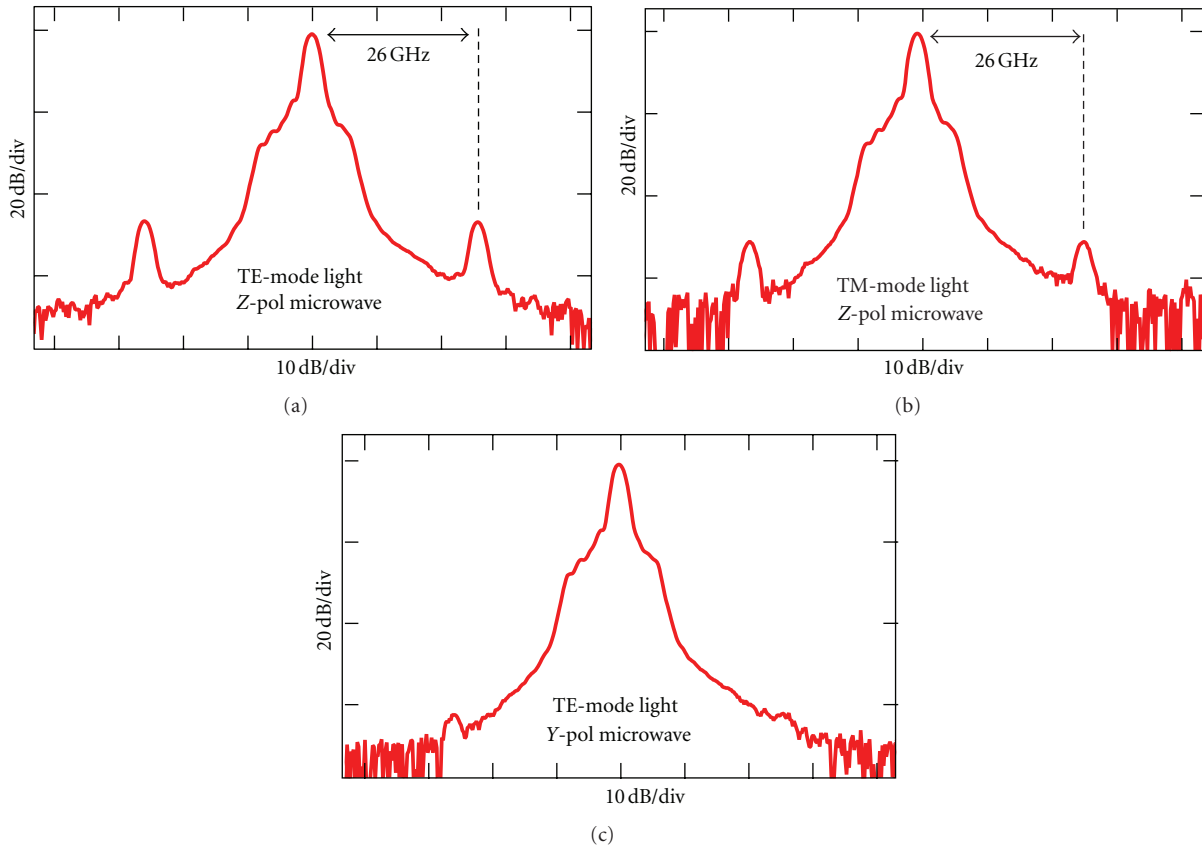


FIGURE 6: Measured output light spectra under microwave wireless signal irradiation of 26 GHz. (a) Output light spectrum for A-polarization of microwave signal and TE-mode of lightwave. (b) Output light spectrum for Z-polarization of microwave signal and TM-mode of lightwave. (c) Output light spectrum for Y-polarization of microwave signal and TE-mode of lightwave.

contributed to the modulation index of the device since the modulation index expresses by the spectrum intensity ratio between the first sideband and the optical carrier. However, low insertion loss is an important issue to realize low power consumption in the wireless-over-fiber system.

6. Conclusions

An x -cut LiNbO_3 optical modulator using gap-embedded patch-antennas was proposed for wireless microwave-lightwave signal conversion in the wireless-over-fiber systems. The proposed device is fabricated on x -cut LiNbO_3

substrate with no buffer layer structure. Modulation efficiency enhancement using the x -cut LiNbO_3 optical modulators can be obtained. The basic operations of the proposed device were demonstrated successfully. The modulation efficiency of the proposed device was enhanced by 6 dB compared to the z -cut LiTaO_3 -based device.

Wireless microwave/millimetre-wave-lightwave signal conversion with extremely low microwave/millimetre-wave signal distortion can be realized by the use of the proposed devices with simple compact structures. By using many gap-embedded patch-antennas in array structure with polarization-reversed structure of the x -cut LiNbO_3 for

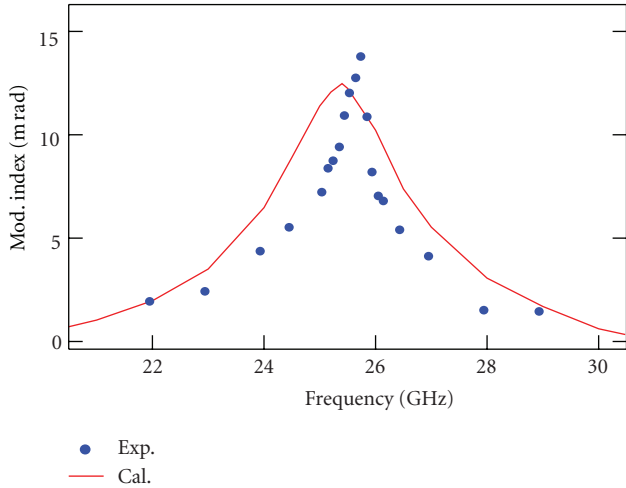


FIGURE 7: Measured frequency dependences of modulation efficiency with wireless irradiation angle of 0 degree (normal direction).

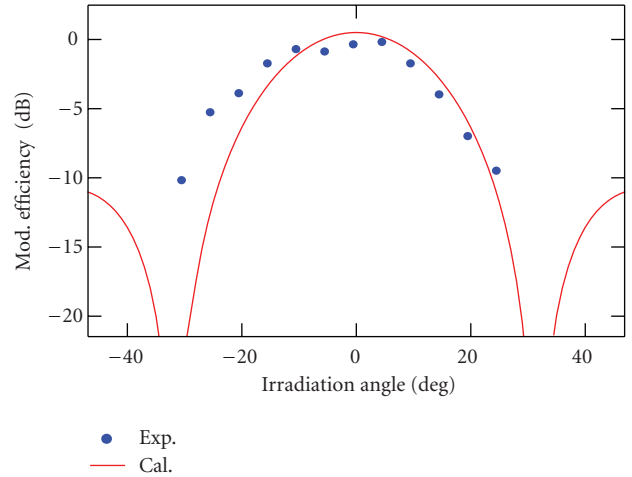


FIGURE 9: Measured wireless irradiation angle dependences (directivity) of modulation efficiency.

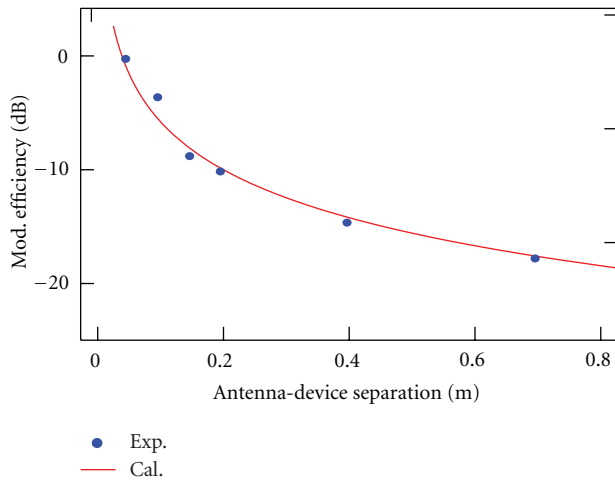


FIGURE 8: Measured antenna-device separation dependences of modulation efficiency.

obtaining quasiphase-matching structures, the modulation efficiency can be further enhanced.

Acknowledgments

The authors would like thanks to Dr. Hidehisa Shiomi and Dr. Kazuhiro Kitatani, from Osaka University, for their precious suggestions throughout the discussion and kind support in the experiment. This research was supported in part by the Grants-in-Aid for Scientific Research and the Grants for Osaka University Global COE Program, Center for Electronics Device Innovation, both from the Ministry of Education, Culture, Sports, Science, and Technology in Japan.

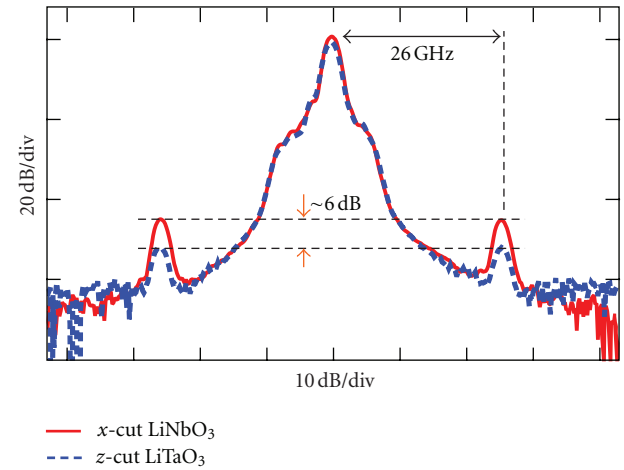


FIGURE 10: Comparison of measured output light spectra using the x-cut LiNbO₃ and z-cut LiTaO₃-based devices.

References

- [1] A. J. Seeds, "Microwave photonics," *IEEE Transactions on Microwave Theory and Techniques*, vol. 50, no. 3, pp. 877–887, 2002.
- [2] S. Iezekiel, *Microwave Photonics: Devices and Applications*, John Wiley & Sons, Chichester, UK, 2009.
- [3] I. Watanabe, T. Nakata, M. Tsuji, K. Makita, T. Torikai, and K. Taguchi, "High-speed, high-reliability planar-structure super-lattice avalanche photodiodes for 10-Gb/s optical receivers," *Journal of Lightwave Technology*, vol. 18, no. 12, pp. 2200–2207, 2000.
- [4] R. Krähenbühl, J. H. Cole, R. P. Moeller, and M. M. Howerton, "High-speed optical modulator in LiNbO₃ with cascaded resonant-type electrodes," *Journal of Lightwave Technology*, vol. 24, no. 5, pp. 2184–2189, 2006.
- [5] S. Shinada, T. Kawanishi, and M. Izutsu, "A resonant type linbo₃ optical modulator array with micro-strip antennas," *IEICE Transactions on Electronics*, vol. E90-C, no. 5, pp. 1090–1095, 2007.

- [6] R. B. Waterhouse and D. Novak, "Integrated antenna/electro-optic modulator for RF photonic front-ends," in *Proceedings of the International Microwave Symposium (WE2C-4 '11)*, Baltimore, Md, USA, June 2011.
- [7] F. T. Sheehy, W. B. Bridges, and J. H. Schaffner, "60 GHz and 94 GHz antenna-coupled LiNbO₃ electrooptic modulators," *IEEE Photonics Technology Letters*, vol. 5, no. 3, pp. 307–310, 1993.
- [8] W. B. Bridges, F. T. Sheehy, and J. H. Schaffner, "Wave-coupled LiNbO₃ electrooptic modulator for microwave and millimeter-wave modulation," *IEEE Photonics Technology Letters*, vol. 3, no. 2, pp. 133–135, 1991.
- [9] H. Murata, R. Miyanaka, and Y. Okamura, "Wireless space-division-multiplexed signal discrimination device using electro-optic modulator with antenna-coupled electrodes and polarization-reversed structures," *International Journal of Microwave and Wireless Technologies*, vol. 4, pp. 399–405, 2012.
- [10] Y. N. Wijayanto, H. Murata, and Y. Okamura, "Electro-optic wireless millimeter-wave-lightwave signal converters using planar Yagi-Uda array antennas coupled to resonant electrodes," in *Proceedings of the Optoelectronics and Communications Conference*, vol. 5E1-2, Busan, Republic of Korea, July 2012.
- [11] Y. N. Wijayanto, H. Murata, and Y. Okamura, "Novel electro-optic microwave-lightwave converters utilizing a patch antenna embedded with a narrow gap," *IEICE Electronics Express*, vol. 8, no. 7, pp. 491–497, 2011.
- [12] Y. N. Wijayanto, H. Murata, and Y. Okamura, "Electro-optic microwave-lightwave converters utilizing patch antennas with orthogonal gaps," *Journal of Nonlinear Optical Physics and Materials*, vol. 21, no. 1, Article ID 1250001, 2012.
- [13] Y. N. Wijayanto, H. Murata, and Y. Okamura, "Electro-optic microwave-lightwave converters utilizing a quasi-phase-matching array of patch antennas with a gap," *Electronics Letters*, vol. 48, no. 1, pp. 36–38, 2012.
- [14] G. Lefort and T. Razban, "Microstrip antennas printed on lithium niobate substrate," *Electronics Letters*, vol. 33, no. 9, pp. 726–727, 1997.
- [15] V. R. Gupta and N. Gupta, "Characteristics of a compact microstrip antenna," *Microwave and Optical Technology Letters*, vol. 40, no. 2, pp. 158–160, 2004.
- [16] R. Rodríguez-Berral, F. Mesa, and D. R. Jackson, "Gap discontinuity in microstrip lines: an accurate semianalytical formulation," *IEEE Transactions on Microwave Theory and Techniques*, vol. 59, no. 6, pp. 1441–1453, 2011.
- [17] R. E. Newnham, *Properties of Materials*, Oxford University Press, New York, 2005.
- [18] A. Yariv, *Quantum Electronics*, Wiley, New York, Ny, USA, 3rd edition, 1989.
- [19] H. Murata, S. Matsunaga, A. Enokihara, and Y. Okamura, "Resonant electrode guided-wave electro-optic phase modulator using polarisation-reversal structures," *Electronics Letters*, vol. 41, no. 8, pp. 497–498, 2005.



Hindawi

Submit your manuscripts at
<http://www.hindawi.com>

